Fluctuations in polymer blends

Dominik Düchs and Friederike Schmid

Fakultät für Physik, Universität Bielefeld, Postfach 100131, 33501 Bielefeld
E-mail: {schmid, duechs}@physik.uni-bielefeld.de

We have developed a new Monte Carlo approach to studying polymer mixtures. The method is applied to symmetrical ternary blends of A and B homopolymers and AB copolymers. Our results are in good agreement with experiments.

1 Introduction

Polymers are large molecules made of a high number of identical ("monomer") units[1]. They play a central role in chemical technology, materials science and even biology. A simple and straightforward way of creating new polymeric materials is to blend different polymer species (A and B) into a single melt. Unfortunately, different organic molecules are usually incompatible, and the incompatibility is amplified in polymers by the number of monomeric units. Therefore, polymers of different type are usually immiscible. The situation can be improved by adding as compatibilizers multicomponent polymers ("copolymers") which contain both types of monomers. Small amounts of compatibilizers stabilize homogeneous mixed phases over a wider range of temperatures. At temperatures where the blend demixes nevertheless, they reduce the interfacial tension between the A- and B-rich regions. If larger amounts of compatibilizers are added, new phases with complex morphologies emerge where A and B domains are separated on a microscopic scale (microphase separation)[2–7].

Theoretical studies of such materials face the problem that orders of magnitude lie between the length scale of an atom and that of a microphase separated domain. Fortunately, some kind of averaging takes place in many polymer systems: Since polymers are in contact with many other polymers, chemical details on the monomer scale largely wash out and can be absorbed into a few effective parameters. This explains the high success of coarse grained models in polymer science. Moreover, the high number of interaction partners ensures that mean-field theories, which ignore the effect of local composition or density fluctuations, have an unusually large range of validity.

However, the regions where mean-field theories fail are sometimes the most interesting. One prominent example is the microemulsion channel in ternary symmetric mixtures of A and B homopolymers, and AB diblock copolymers (see Fig. 1). A mean-field phase diagram for such a system is shown in Fig. 2 (left) as a function of the homopolymer volume

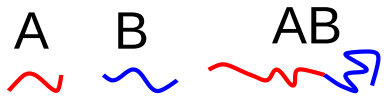

Figure 1. Schematic picture of the components of a ternary A+B+AB polymer blend.

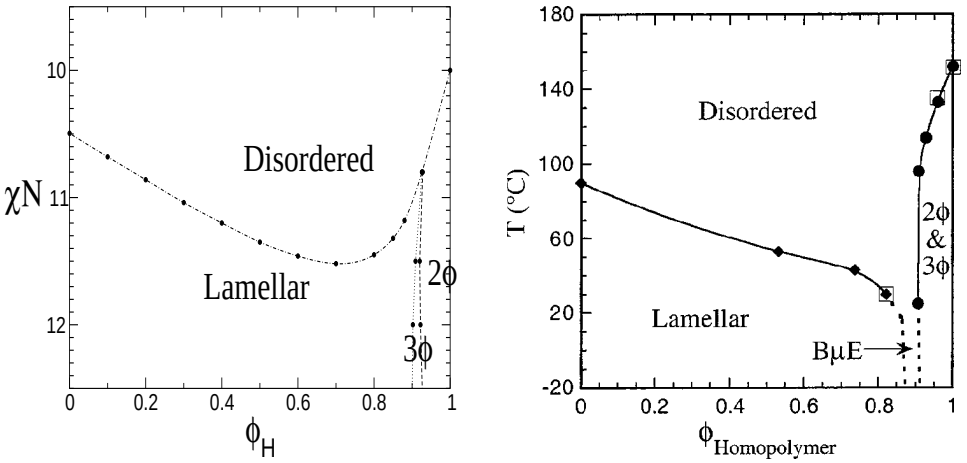

Figure 2. Phase diagrams of the ternary A+B+AB blend as a function of the homopolymer volume fraction Φ_H. The chain length of the copolymers is roughly five times that of the homopolymers. See text for the explanation of the phases. Left: Mean field phase diagram as a function of the monomer incompatibility parameter χ, multiplied with the copolymer chain length N. Right: Experimental phase diagram of a PDMS+PEE+PDMS-PEE blend as a function of temperature. After Ref. 7. Reproduced by permission of The Royal Society of Chemistry.

fraction Φ_H and the polymer incompatibility χN (χ is a measure for the incompatibility of A and B monomers, and N the number of monomers in the copolymer). Four different phases are predicted: A completely mixed ("Disordered") phase, an ordered ("Lamellar") phase which contains of alternating A- and B-sheets, and a region where two A-rich and B-rich phases separate on a macroscopic scale ("2 Φ"). 3Φ denotes a region of coexistence between three phases: the lamellar phase, the A-rich phase, and the B-rich phase.

The mean-field theory thus predicts the existence of a point where the lamellar phase, the disordered mixed phases and the A-rich and B-rich phase meet. Such a point is called an isotropic Lifshitz point (LP)[10]. The thickness of the lamellar sheets there reaches infinity. It is intuitive that this mean-field prediction is likely to fail in real systems: If the lamellar distance is large enough that the interfaces between A and B sheets can bend around (i. e., larger than the "persistence length" of the interfaces), one might expect that the lamellae rupture and form a globally disordered structure. These arguments are supported by the theoretical result that the mean-field lower critical dimension of isotropic LPs is four[9], implying that LPs are probably destroyed by fluctuations in three dimensions (unfortunately, the true value of the lower critical dimension is not known).

Indeed, experimental phase diagrams differ substantially from the mean-field phase diagram. An example due to Hillmyer et al[7] is shown in Fig. 2 (right). In the experiments, the LP is destroyed, the three phase coexistence between the lamellar phase and the A- and B-rich phase is removed and replaced by a macroscopically mixed phase. This phase is locally microphase separated into A- and B-domains, but the domains are interconnected and form a globally disordered bicontinuous network. ("Bicontinuous" means that infinitely extended connected A- and B-clusters exist in all space directions.)

Such bicontinuous alloys are very interesting for applications. They are able to reproduce certain useful properties of the individual components such as conductivity or

permeability. In addition, they often have particularl nice mechanical properties[8]. In order to study them theoretically, one has to go beyond mean-field theory and study the influence of fluctuations on the phase behavior of the blend.

Analytical polymer theories are most commonly based on the Edwards model[11], a very elegant model which eliminates microscopic details entirely, and describes polymers by only a few phenomenological parameters. It will be described briefly in section 2.1. This model has been used to calculate the mean-field phase diagram in Fig. 2.

In contrast, computer simulations often use particle-based models, where the polymers are represented by chains of idealized coarse-grained units. Such systems still exhibit local structure, which may even differ quite substantially from that of the real polymer blend. The approach is of course justified by the fact that microscopic details should not matter, in the end. Nevertheless, a simulation of the original Edwards model seems desirable. It allows to assess most directly the influence of fluctuations, e. g., on the phase diagram of Fig. 2.

Motivated by these considerations, we have designed and tested a new Monte Carlo simulation method for polymer blends, which aims at a direct simulation of the Edwards model. As a first application, we have used the method to study ternary A+B+AB polymer blends in two dimensions. We found that the Edwards model indeed reproduces the features of the experimental phase diagram, Fig. 2 (right), once fluctuations are taken into account. In particular, we recover the microemulsion channel[12,13].

The present paper reviews some of these results. The remainder of it is organized as follows. The theory and the numerical method will be outlined in Sec. 2. The results will be presented in Sec. 3.

2 Theory and Method

Due to lack of space, we can only give a very incomplete account of the simulation method and the underlying theory. The interested reader is referred to Refs. 12, 13 for a more detailed presentation.

2.1 The Gaussian chain model

In the Edwards model, (linear) polymers are represented by "Gaussian chains": continuous paths in space subject to a harmonic stretching energy. In statistical averages over polymer conformations, each possible polymer path $\mathbf{R}(s)$ (with $s \in [0, N]$, N being the chain length or total number of monomers in the chain) thus carries an *a priori* Gaussian statistical weight

$$\mathcal{P}\{\mathbf{R}\} = \mathcal{N} \exp\left[\frac{3}{2b^2}\int_0^N ds \left|\frac{d\mathbf{R}(s)}{ds}\right|^2\right], \tag{1}$$

where $\mathcal{N}$ is the normalization factor and b a phenomenological parameter, the statistical segment length. The latter is related to the typical extension of a non-interacting Gaussian chain, the "radius of gyration", via

$$R_g = b\sqrt{N/2d}, \tag{2}$$

where d is the space dimension. For simplicity, we take b to be identical for all monomer species.

We consider incompressible blends of (co)polymers made of two monomer species A and B. The incompressibility condition implies that the total monomer density, defined as

$$\hat{\Phi}(\mathbf{r}) = \frac{1}{\rho_0} \sum_i \int ds\, \delta(\mathbf{r} - \mathbf{R}_i(s)), \tag{3}$$

is constant everywhere, $\hat{\Phi} \equiv 1$. Here the sum i runs over all (co)polymers, and $1/\rho_0$ is the volume per monomer, also taken to be identical for A and B monomers for simplicity. The chemistry of a given (co)polymer can formally be described by a monomer distribution function $\gamma(s)$ ($s \in [0 : N]$), which is one if the s-th monomer is of type A, and zero otherwise. For example, A-homopolymers are characterized by $\chi \equiv 1$ and B-homopolymers by $\chi \equiv 0$. The local density of A-monomers is then given by

$$\hat{\Phi}_\alpha(\mathbf{r}) = \frac{1}{\rho_0} \sum_i N_i \int ds\, \gamma_i(s)\, \delta(\mathbf{r} - \mathbf{R}_j(s)), \tag{4}$$

and that of B-monomers by $\phi_B = \hat{\Phi} - \hat{\Phi}_A$.

In addition to the unspecific interactions which cause the polymers to aggregate into an incompressible blend, we also have a small relative repulsion between A and B monomers which drives the phase segregation. The latter is modeled as a local contact interaction with the interaction energy

$$H_I = \chi\rho_0 \int d\mathbf{r}\, \hat{\Phi}_A(\mathbf{r})\, \hat{\Phi}_B(\mathbf{r}). \tag{5}$$

The parameter χ is the second phenomenological parameter of the theory, the Flory-Huggins parameter.

Putting it all together, the canonical partition function of the system is

$$\mathcal{Z}_c \propto \int \prod_i \mathcal{D}\mathbf{R}_i \mathcal{P}\{\mathbf{R}\} \delta(\hat{\Phi} - 1) \exp(-H_I), \tag{6}$$

where $\int \mathcal{D}\mathbf{R}$ denotes a path integral over the chain conformations.

2.2 Fluctuating fields

The expression (6) for the partition function is not very handy for practical (analytical or numerical) calculations. To proceed further, it is convenient to decouple the integrals over different paths by means of a Hubbard-Stratonovich transformation[14]. One obtains a functional integral over a set of imaginary fields W_+, which are conjugate to the total density $\hat{\Phi}$, and real fields W_-, which are conjugate to the density difference $\hat{m} = \hat{\Phi}_B - \hat{\Phi}_A$:

$$\mathcal{Z} \propto \int_\infty \mathcal{D}W_- \int_{i\infty} \mathcal{D}W_+ \exp(-H_C). \tag{7}$$

with

$$H_C(W_-, W_+) = C\Big[\frac{1}{\chi N} \int d\mathbf{r}\, W_-^2 - \int d\mathbf{r}\, W_+ - \sum_j V_j \frac{N}{N_j} \ln \mathcal{Q}_j\Big]. \tag{8}$$

Here N denotes some reference chain length – in our case the length of the copolymer. The global prefactor is $C = \rho_0/N$, V_j is the partial volume occupied by all polymers of type j, N_j their chain length, and $\mathcal{Q}_j$ their single chain partition function in the external field $W_\pm$:

$$\mathcal{Q}_j = \int d\mathbf{r}\; q_j(\mathbf{r}, N_j), \tag{9}$$

where the propagators q_j satisfy the diffusion equation

$$\frac{\partial}{\partial s} q_j(\mathbf{r}, s) = \frac{1}{N}[\Delta - W(\mathbf{r}, s)]\; q_j(\mathbf{r}, s) \qquad q_j(\mathbf{r}, 0) = 1 \tag{10}$$

with $W(\mathbf{r}, s) = W_+(\mathbf{r}) + (2\gamma(s) - 1)W_-(\mathbf{r})$. Here and throughout the paper, all lengths are expressed in units of the radius of gyration (2) of an ideal chain of length N.

A similar calculation can be performed for the grand canonical partition function. The partition function has the same form as in (7) with H_C replaced by

$$H_{GC}(W_-, W_+) = C\Big[\frac{1}{\chi N}\int d\mathbf{r}\; W_-^2 - \int d\mathbf{r}\; W_+ - \sum_j z_j \mathcal{Q}_j\Big], \tag{11}$$

where z_j is the fugacity of the polymer species j.

Eq. (7) is often the starting point for self-consistent field theories. In that approach, the integral is approximated by its saddle point, i. e., the energy functional (8) is minimized. This leads to a self-consistent set of equations, which are solved by *real* fields W_+ and W_-. The self-consistent field theory becomes exact in the limit $C \to \infty$. The parameter C thus acts as a "Ginzburg parameter", which can be used to turn the fluctuations on and off. In our simulations, we used $C = 50$.

2.3 Monte Carlo simulations

Our work aimed at going beyond the mean-field theory and evaluating the integral (7) by Monte Carlo integration, with the Metropolis algorithm[15]. The sampling of the real fields W_- was straightforward. In the case of the imaginary fields W_+, we presumed that the integral is still dominated by the local saddle point $\bar{W}_+$ (which depends on W_- and deformed the integration path such that it passes through $\bar{W}_+$.

$$\int_{i\infty} \mathcal{D}W_+ \cdots = \int_{\bar{W}_+ + i\infty} \mathcal{D}W_+ \cdots ,$$

The (complex) argument of the integral in (7) was split into a real part $\exp(-H_C^R)$, which enters the Metropolis algorithm, and a complex reweighting factor I_C. Note that the latter is non-positive-definite, an example for a "sign problem" as is well-known from other branches of physics[16]. Fortunately, we could show that I_C is uncorrelated with W_-, and that $\exp(-H_C^R[W_+])$ is virtually identical with the analogous quantity $\exp(-H_C[\bar{W}_+])$. In most simulation runs, we have therefore replaced the integral over W_+ by the saddle point $\bar{W}_+$.

Alternative ways of sampling Eq. (7) are also possible. In particular, Fredrickson and coworkers have successfully implemented and explored the method of complex Langevin simulations[17,18]. Parallel to our simulations of the ternary A+B+AB blend, Ganesan and

Fredrickson have examined the same system with the complex Langevin method. It turned out that our Monte Carlo method was better suited to study that specific system, in the sense that a larger portion of the phase diagram could be investigated reliably. In the regions where both methods worked well, the agreement was very good[13].

2.4 Technical details

Every Monte Carlo step involved the calculation of a saddle point $\bar{W}_+$ for fixed W_-. This was done by iteration of the self-consistent equations, employing a two-step Anderson mixing scheme[19]. The iteration was terminated once $\Delta H < 0.001$. This typically required roughly 10 iteration steps. The most time-consuming part was the solution of the diffusion equation (10). Here, we used a pseudo-spectral method[20] which has been developed originally to solve the Schrödinger equation, in combination with highly optimized Fast Fourier Transform routines[21].

3 Results

3.1 Phase behavior of a ternary A+B+AB blend

We have used the method described in the previous section, to re-examine the phase behavior of the system of Fig. 2: A ternary symmetrical A+B+AB mixture with copolymers five times as long as the homopolymers. To keep the computational costs low, we performed this first study in two dimensions only.

We begin with showing configuration snapshots for some of the parameters. The propagators obtained from Eq. (10), together with their conjugate propagators $q_j^\dagger$, which propagate from the opposite end of the polymer, can be used to calculate the density functions

$$\bar{\Phi}_A(\mathbf{r}) = \sum_j \frac{V_j}{\mathcal{Q}_j N_j} \int_0^{N_j} ds\, q_j(\mathbf{r},s)\, q_j^\dagger(\mathbf{r},s)\, \gamma_j(s) \tag{12}$$

$$\bar{\Phi}_B(\mathbf{r}) = \sum_j \frac{V_j}{\mathcal{Q}_j N_j} \int_0^{N_j} ds\, q_j(\mathbf{r},s)\, q_j^\dagger(\mathbf{r},s)\, (1-\gamma_j(s)). \tag{13}$$

These depend on $W_\pm$ and are in general complex. Nevertheless, their ensemble averages yield real densities which correspond to experimentally measurable quantities. If W_+ is replaced by $\bar{W}_+$, the $\bar{\Phi}_A$ and $\bar{\Phi}_B$ are real already for single configurations, and can be used to visualize them.

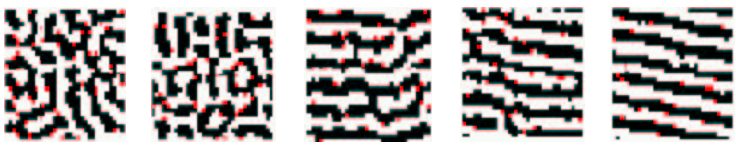

Figure 3. Snapshots for pure copolymer systems at χN = 11.1, 11.2, 11.3, 11.4, 11.5. White pixels: $0 < \bar{\Phi}_A < 0.49$, red pixels:$0.49 < \bar{\Phi} < 0.51$, black pixels: $0.51 < \bar{\Phi} < 1$.

Figure 4. Snapshots for ternary mixtures with homopolymer volume fraction $\Phi_H = 0.7$ at χN = 12.2, 12.3, 12.4, 12.5.

Figure 5. Snapshots for ternary mixtures with homopolymer volume fraction $\Phi_H = 0.85$ at χN = 12.5, 12.7, 13.0, 13.2.

Fig. 3 shows a series of snapshots at different χN for systems containing copolymers only. All runs were started from a disordered configuration. Beyond polymer incompatibilities $\chi N \approx 11.3$, the copolymers spontaneously assemble into an ordered lamellar structure. Upon adding homopolymer, one finds that the transition shifts to higher χN. This is demonstrated by the snapshots of Figs. 4 and 5 (these runs were started from ordered lamellar configurations).

Based on such configuration images, quantities ("order parameters") can be defined which distinguish between ordered and disordered states. Fig. 6 (left) shows examples of such quantities, their definition can be found in Ref. 13. They were used to localize the order/disorder transition. This worked nicely up to $\Phi_H = 0.85$.

At homopolymer concentrations beyond $\Phi_H \approx 0.9$, a different type of phase transition

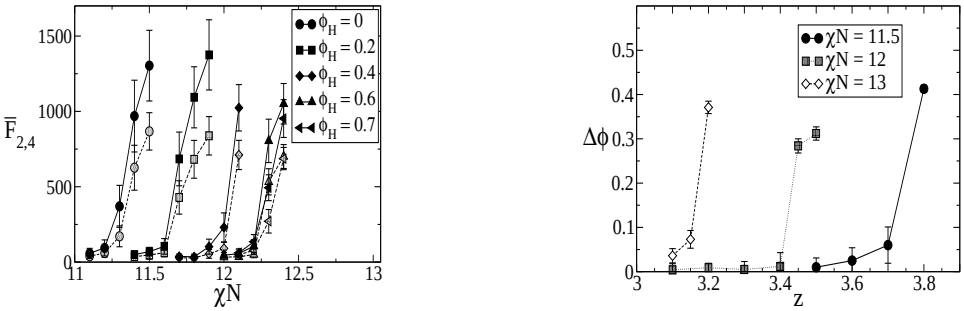

Figure 6. Order parameters for the phase transitions in our System. Left: Quantities $\bar{F}_2$ and $\bar{F}_4$ which serve as order parameter for the order disorder transition, plotted as a function of χN for different homopolymer volume fractions Φ_H. Right: Difference $\Delta\Phi$ in A and B monomer densities, plotted as a function of the relative homopolymer fugacity z, in the grand canonical ensemble.

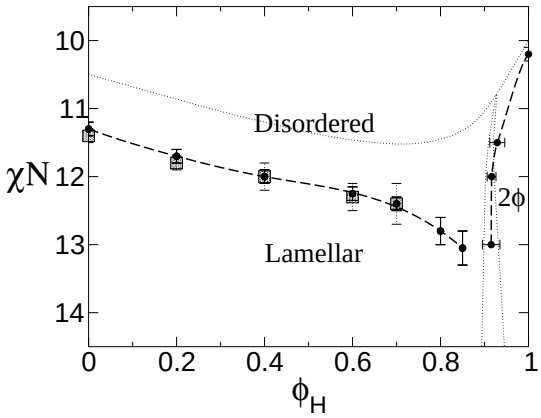

Figure 7. Phase diagram as obtained from the simulations. The circles show the results from the Monte Carlo simulations, the squares those from the complex Langevin simulations for comparison. The dotted lines indicate the mean-field phase boundaries.

is observed: The demixing of an A-rich and a B-rich phase. This transition is best examined in the grand canonical ensemble. In the demixed phase, the A/B symmetry is broken and the overall difference in A and B densities becomes nonzero. The quantity $\Delta\Phi = \Phi_A - \Phi_B$ may thus be used as an order parameter for the transition (Fig. 6, right).

Gathering all our results, we can construct the phase diagram of the system. It is shown in Fig. 7, together with the mean-field phase diagram of Fig. 2. As expected, the fluctuations destroy the Lifshitz point. In the χN-range examined by us, the lamellar phase no longer coexists with demixed A- or B-rich phases. Instead, a bicontinuous disordered microemulsion phase intrudes between these two. The cusp-like shape of the microemulsion region is in good qualitative agreement with the experiments of Fig. 2. To our knowledge, it has here been reproduced for the first time in simulations. We should note that the experimental system is of course three dimensional, while the simulations were carried out in two dimensions. Fluctuation effects are generally stronger in two dimensions than in three dimensions. However, in view of the discussion in the introduction, we expect that the qualitative features of the phase diagram will persist in three dimensions.

For comparison, Fig. 7 also shows data points obtained by Ganesan and Fredrickson with the Complex Langevin method. As mentioned earlier, the agreement is very good.

3.2 Structure of the microemulsion

To further characterize the formation of the microemulsion phase, we have compared the characteristic lamellar distance L_0 with the average curvature diameter D_C of the microdomain boundaries. The order/disorder transition occurs almost precisely at the parameter values where the two become equal. This corroborates our earlier hypothesis on the mechanism by which fluctuations generate the microemulsion phase: It forms when the width of the lamellae grows larger than the curvature diameter of the fluctuating boundaries.

Having established the phase diagram, it is instructive to inspect the local structure of

the fluid in more detail. In amphiphilic systems such as our block copolymer system, the disordered phase is often subdivided into a "microemulsion" region and a "disordered" region, which are separated by a so-called "Lifshitz line"[2]. The property which distinguishes the microemulsion from an ordinary fluid is the presence of a characteristic length scale for composition oscillations, i. e., microemulsions exhibit some kind of local order. For example, such characteristic local composition oscillations are clearly present in the configurations of Figs. 3, 4, and 5. We have determined the rough position of the Lifshitz line for the homopolymer concentration $\Phi_H = 0.82$ and found that the disordered fluid remains structured up to $\chi N \approx 10 - 11$[12,22].

A closer look at Figs. 4 and 5 suggests that this well-known classification may not be sufficient to fully characterize the disordered fluid. At low homopolymer concentration, the structure of the disordered microemulsion resembles that of a "defective lamellar phase". The lamellae have a fixed distance, and disorder is introduced into the system by numerous localized defects. At higher homopolymer concentration, the situation changes. The lamellar distance increases, and the boundaries separating A-rich and B-rich domains fluctuate strongly. These fluctuations eventually destroy the lamellar order. In view of the discussion in the introduction, it is tempting to categorize the resulting microemulsion in this region as a "genuine" microemulsion.

So far, this distinction is merely qualitative. However, it turns out that it is indeed possible to separate two such regimes by a quantitative argument: In the "defective lamellar" region, the characteristic length scale of the fluid is identical to the mean-field lamellar distance. In the "genuine microemulsion" region, the two differ substantially[12,22].

4 Summary

In sum, we have established a novel Monte Carlo method, which allows to study blends of polymers and copolymers by simulation of a fluctuating field theory for polymers. The starting point is the Gaussian chain model for incompressible polymer mixtures, one of the most commonly used models in self-consistent field calculations. Our method allows to investigate the effect of fluctuations on the structure and phase behavior of such blends. Composition fluctuations can be studied exactly. Unfortunately, the incorporation of density fluctuations was hampered by a "sign problem", which we could not truly overcome. Fortunately, we were able to assess the effect of these fluctuations, and show that they do not influence the structure of the blends.

Using the new approach, we have studied the formation of a microemulsion channel in ternary symmetrical blends of A and B homopolymers, and AB diblock copolymers. In agreement with recent experiments and in contrast to the predictions of mean-field theory, we observe the intrusion of a bicontinuous "microemulsion channel" between the lamellar phase and the demixed A and B-rich phases.

We anticipate that our method may become a useful tool to be used in combination with classical self-consistent field theories. The theoretical description by means of self-consistent field calculations is perfectly adequate and quantitatively reliable for most (co)polymer blends. Only in selected regions of the parameter space, the structure of the blend is seriously affected by fluctuations. These can then be studied with field theoretic Monte Carlo simulations.

Acknowledgments

We have very much enjoyed a fruitful collaboration with V. Ganesan and G. Fredrickson, who contributed the complex Langevin simulations. In addition, we have benefitted from discussions with M. Schick. R. Netz, M. Matsen, and S. Sides. This work was supported by the Deutsche Forschungsgemeinschaft. The Monte Carlo simulations were carried out on the CRAY T3E of the NIC institute at the research center Jülich.

References

1. P. Flory, *Principles of Polymer Chemistry* (Cornell University Press, Ithaca, New York, 1979).
2. R. Holyst and M. Schick, J. Chem. Phys. **96**, 7728 (1992).
3. M. Müller and M. Schick, J. Chem. Phys. **105**, 8282 (1996).
4. P. K. Janert and M. Schick, Macromolecules **30**, 3916 (1997).
5. F. S. Bates, W. W. Maurer, P. M. Lipic, M. A. Hillmyer, K. Almdal, K. Mortensen, G. H. Fredrickson, and T. P. Lodge, Phys. Rev. Lett. **79**, 849 (1997).
6. T. L. Morkved, B. R. Chapman, F. S. Bates, T. P. Lodge, P. Stepanek, and K. Almdal, Faraday Discussions **112**, 335 (1999).
7. M. A. Hillmyer, W. W. Maurer, T. P. Lodge, F. S. Bates, and K. Almdal, J. Chem. Phys. **103**, 4814 (1999).
8. G. Holden, N. R. Legge, R. P. Quirk, and H. E. Schroeder, Eds.; *Thermoplastic Elastomers* (Hanser, Cincinnati, 1996).
9. A. Koudlay, Dissertation Universität Halle, 2002.
10. R. M. Hornreich J. Magn. Magn. Mat. **15**, 387 (1980).
11. M. Doi and S. F. Edwards, *The Theory of Polymer Dynamics* (Clarendon, Oxford, 1986).
12. D. Düchs, Dissertation Universität Bielefeld, 2003.
13. D. Düchs, V. Ganesan, G. Fredrickson, and F. Schmid, Macromolecules, in print (2003).
14. J. Zinn-Justin, *Quantum Field Theory and Critical Phenomena* (Clarendon, Oxford, 1993).
15. N. Metropolis, A. W. Rosenbluth, M. N. Rosenbluth, M. N. Teller, A. M. Teller, and E. Teller, J. Chem. Phys. **21**, 1087 (1953).
16. W. J. Schoenmaker, Phys. Rev. D **36**, 1859 (1987).
17. V. Ganesan and G. H. Fredrickson, Europhys. Lett. **55**, 814 (2001).
18. G. H. Fredrickson, J. Chem. Phys. **117**, 6810 (2002).
19. V. Eyert, J. Comp. Phys. **124**, 271 (1996).
20. M. D. Feit, J. A. Fleck, Jr. and A. Steiger, J. Comp. Phys. **47**, 412 (1982).
21. M. Frigo and S. G. Johnson, *The Fastest Fourier Transform in the West 2.1.3*, (MIT, Cambridge, MA, 2000, software package freely downloadable from www.fftw.org).
22. D. Düchs, F. Schmid, in preparation (2003).